US 20240110301A1

(19) **United States**

(12) **Patent Application Publication**

Cerron Calle et al.

(10) **Pub. No.: US 2024/0110301 A1**

(43) **Pub. Date: Apr. 4, 2024**

(54) **COBALT-COPPER NANOENABLED ELECTRODES**

(71) Applicants: **Gabriel Cerron Calle**, Tempe, AZ (US); **Ana dos Santos Fajardo**, Marinha Grande (PT); **Sergio Garcia-Segura**, Tempe, AZ (US); **Carlos M. Sanchez**, Paris (FR)

(72) Inventors: **Gabriel Cerron Calle**, Tempe, AZ (US); **Ana dos Santos Fajardo**, Marinha Grande (PT); **Sergio Garcia-Segura**, Tempe, AZ (US); **Carlos M. Sanchez**, Paris (FR)

(21) Appl. No.: **18/321,991**

(22) Filed: **May 23, 2023**

Related U.S. Application Data

(60) Provisional application No. 63/344,749, filed on May 23, 2022.

Publication Classification

(51) **Int. Cl.**

C25B 11/077	(2006.01)
C25B 1/27	(2006.01)
C25B 11/031	(2006.01)
C25B 11/061	(2006.01)

(52) **U.S. Cl.**

CPC ***C25B 11/077*** (2021.01); ***C25B 1/27*** (2021.01); ***C25B 11/031*** (2021.01); ***C25B 11/061*** (2021.01)

(57) **ABSTRACT**

A nanocomposite electrode includes a porous copper substrate, Co_3O_4 and/or $Cu/Co(OH)_x$ nanoparticles electrolytically deposited on the porous copper substrate. Fabricating the nanocomposite electrode includes contacting the porous copper substrate with a solution comprising cobalt, and electrodepositing the cobalt on the porous copper substrate to yield the nanocomposite electrode. Reducing nitrate to ammonia includes contacting the nanocomposite electrode with an aqueous solution comprising nitrate, and electrocatalytically reducing the nitrate to yield ammonia.

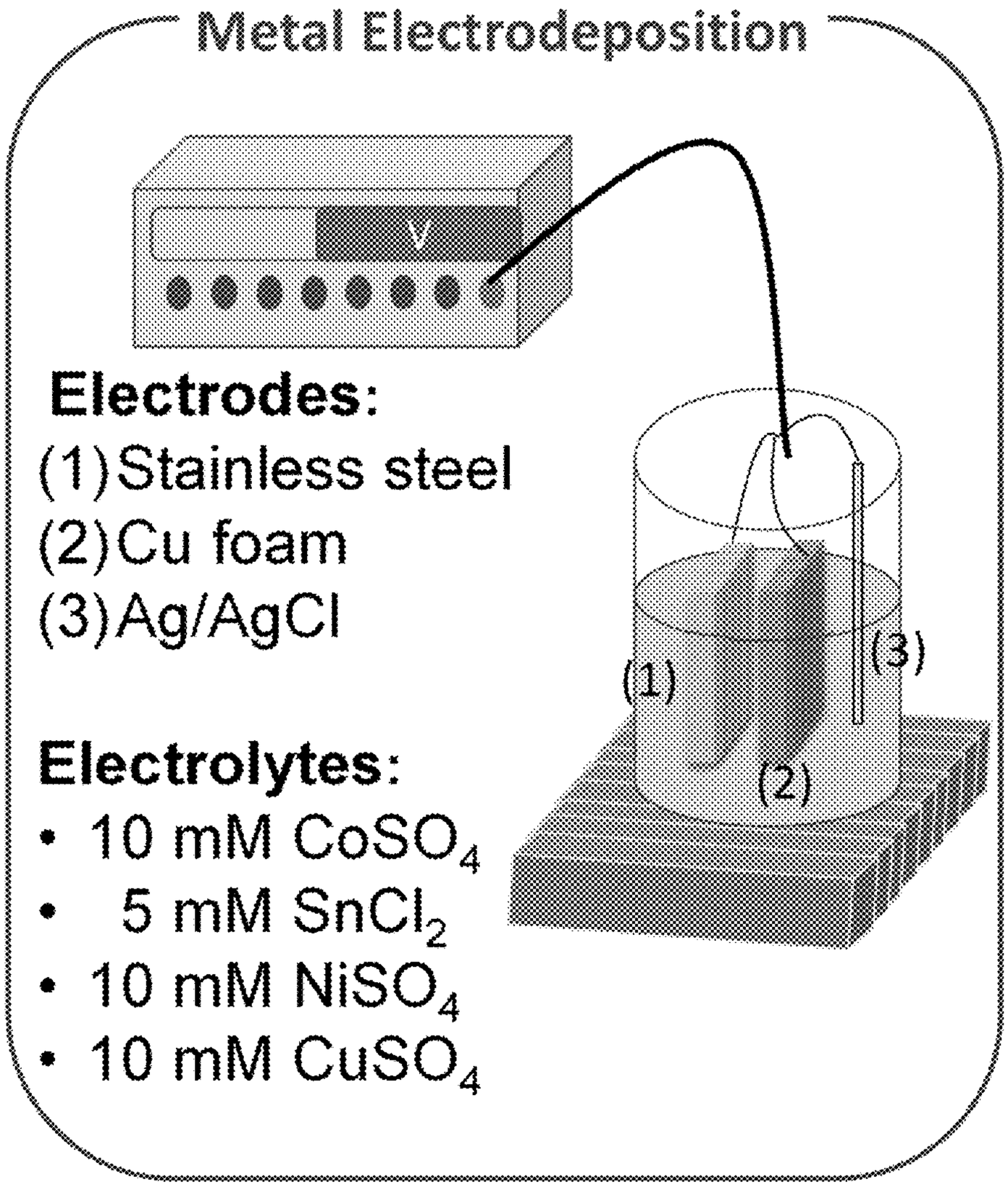

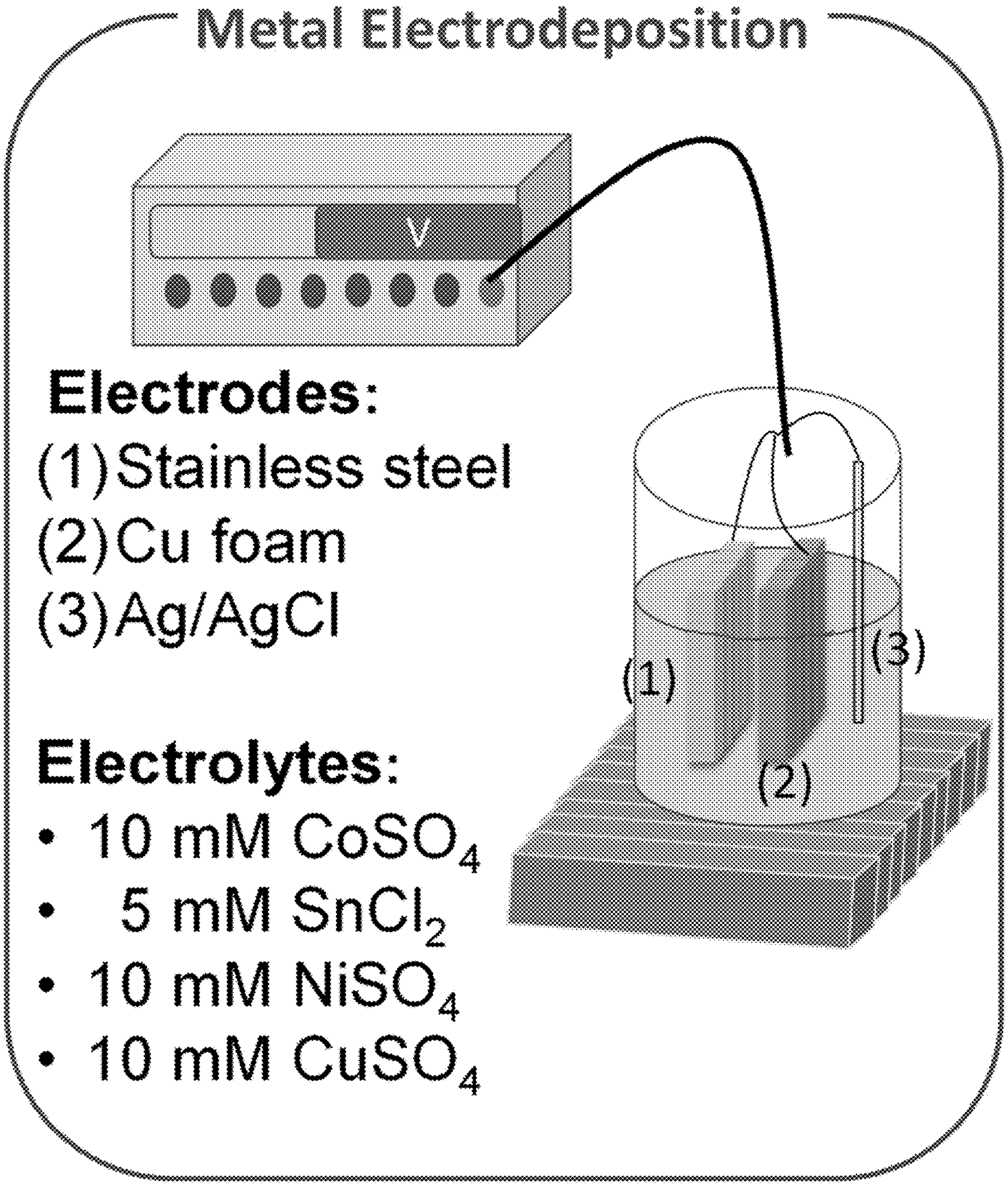
Metal Electrodeposition
V
Electrodes:
(1) Stainless steel
(2) Cu foam
(3) Ag/AgCl
Electrolytes:
• 10 mM $CoSO_4$
• 5 mM $SnCl_2$
• 10 mM $NiSO_4$
• 10 mM $CuSO_4$
(1)
(2)
(3)

FIG. 1A

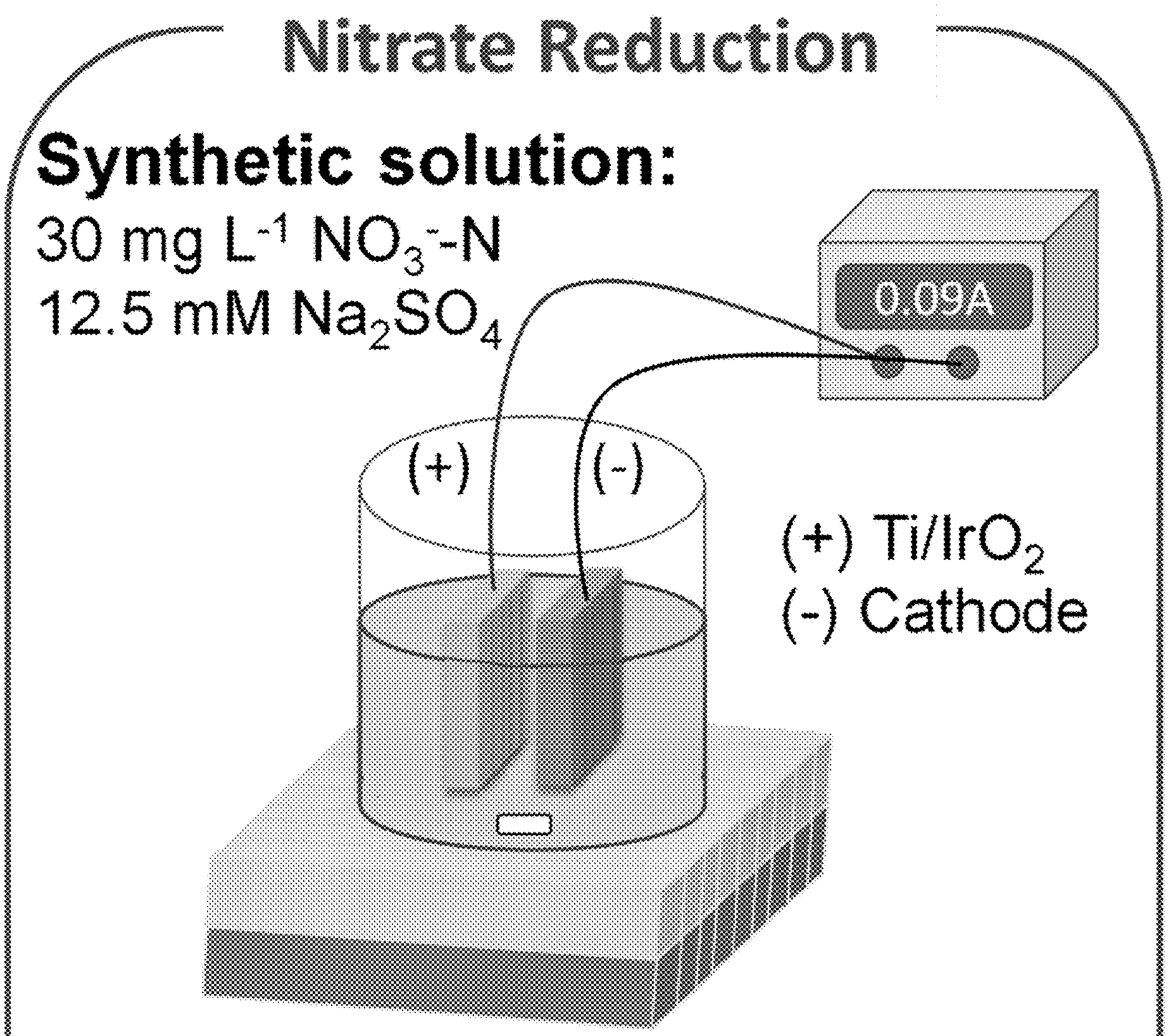
Nitrate Reduction
Synthetic solution:
30 mg L-1 NO3--N
12.5 mM Na2SO4
0.09A
(+)
(-)
(+) Ti/IrO2
(-) Cathode
Nitrate reduction was monitored every 0, 30, 60,120, 180, 240 minutes using HACH kits to measure NO3-, NO2- and NH3

FIG. 1B

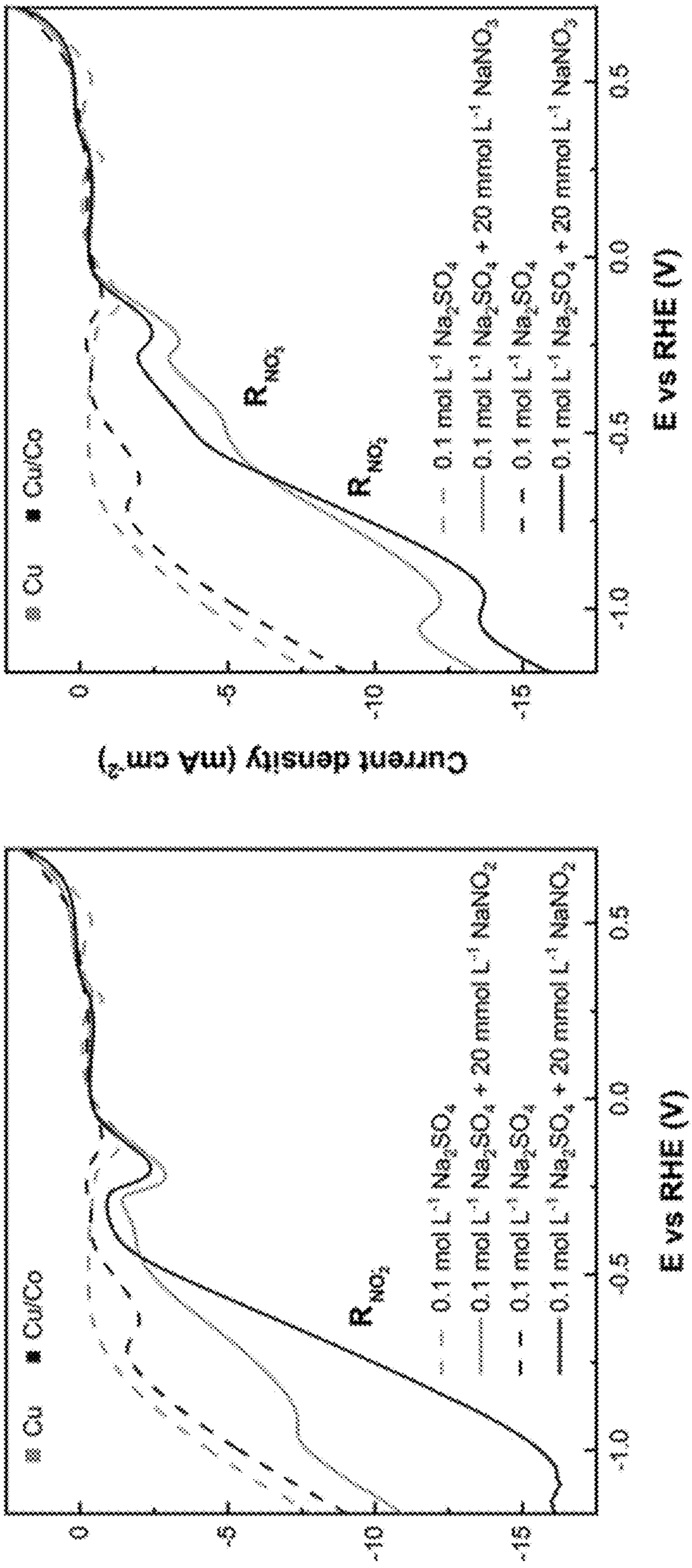
Cu
CuCo
$R_{NO_2^-}$
$R_{NH_4^+}$
0.1 mol L⁻¹ Na₂SO₄
0.1 mol L⁻¹ Na₂SO₄ + 20 mmol L⁻¹ NaNO₂
Current density (mA cm⁻²)
E vs RHE (V)
0
-5
-10
-15
0.5
0.0
-0.5
-1.0

FIG. 2B

FIG. 2A

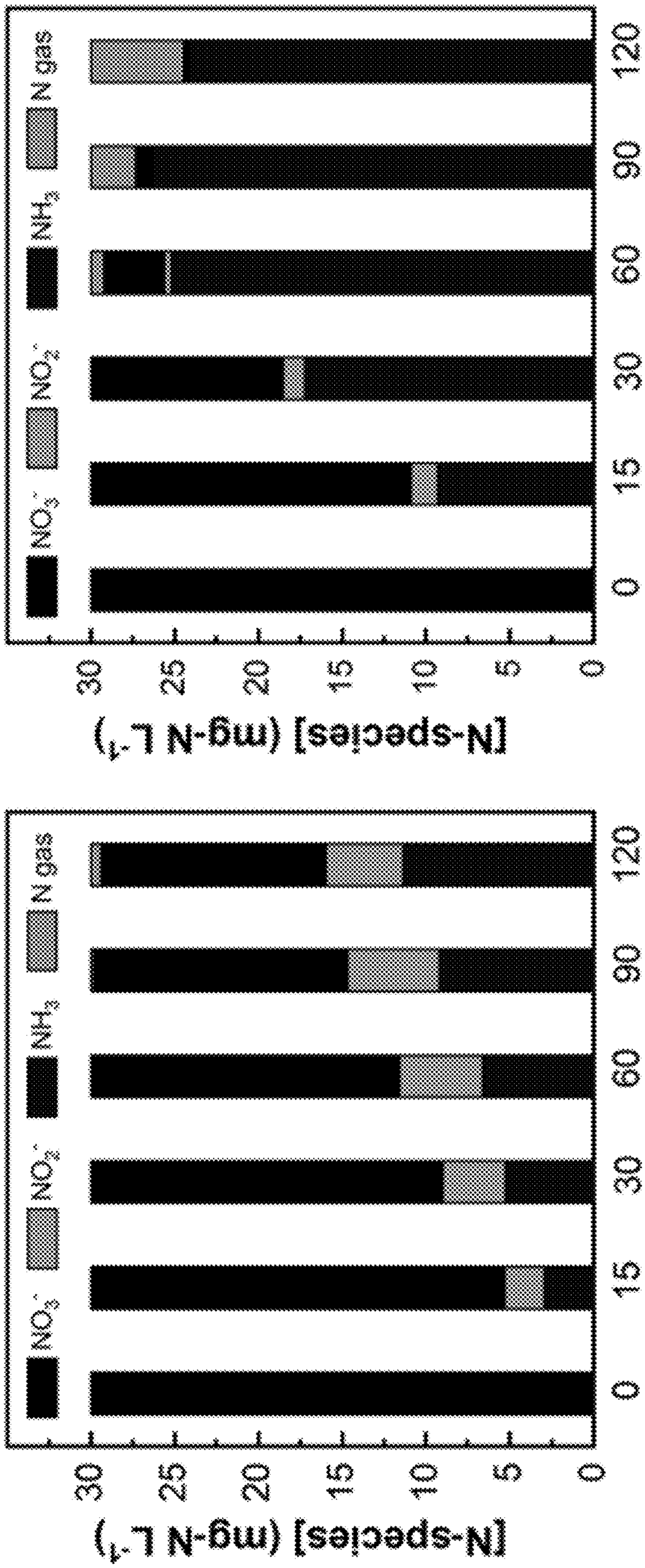
N gas
NH_3
NO_2^-
NO_3^-
0
15
30
60
90
120
Time (min)
0
5
10
15
20
25
30
[N-species] (mg-N L^{-1})

FIG. 3B

NH_3
N gas
NO_2^-
NO_3^-
0
15
30
60
90
120
Time (min)
0
5
10
15
20
25
30
[N-species] (mg-N L^{-1})

FIG. 3A

FIG. 4A

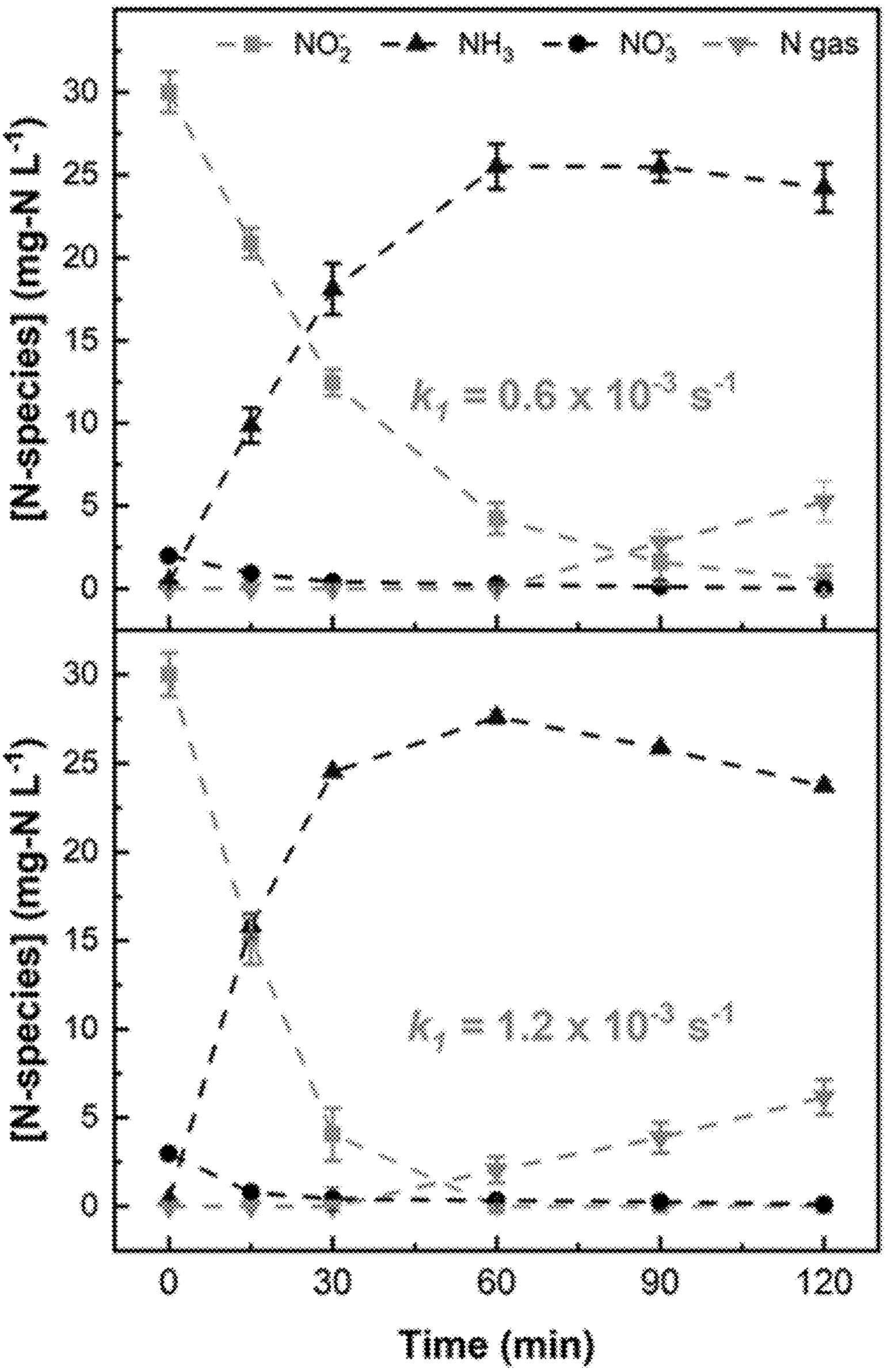
NO_2^-
NH_3
NO_3^-
N gas
[N-species] (mg-N L^{-1})
$k_1 = 0.6 \times 10^{-3}$ s^{-1}
$k_1 = 1.2 \times 10^{-3}$ s^{-1}
0
5
10
15
20
25
30
0
30
60
90
120
Time (min)

FIG. 4B

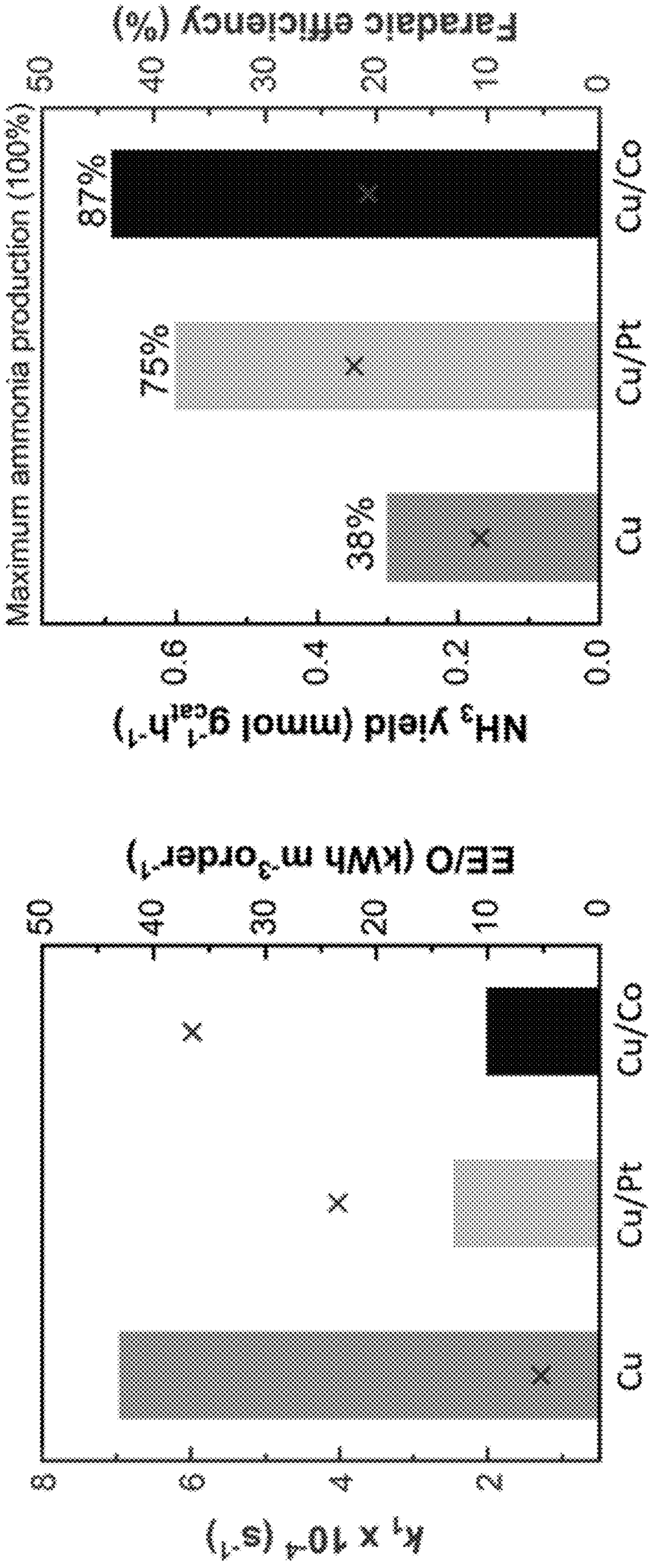
Faradaic efficiency (%)
50
40
30
20
10
0
87%
75%
38%
Cu/Co
Cu/Pt
Cu
Electrode
Maximum ammonia production (100%)
NH3 yield (mmol gcat-1h-1)
0.6
0.4
0.2
0.0
EE/O (kWh m-3order-1)
50
40
30
20
10
0
Cu/Co
Cu/Pt
Cu
Electrode
k1 x 10-4 (S-1)
8
6
4
2

FIG. 5B

FIG. 5A

FIG. 6A

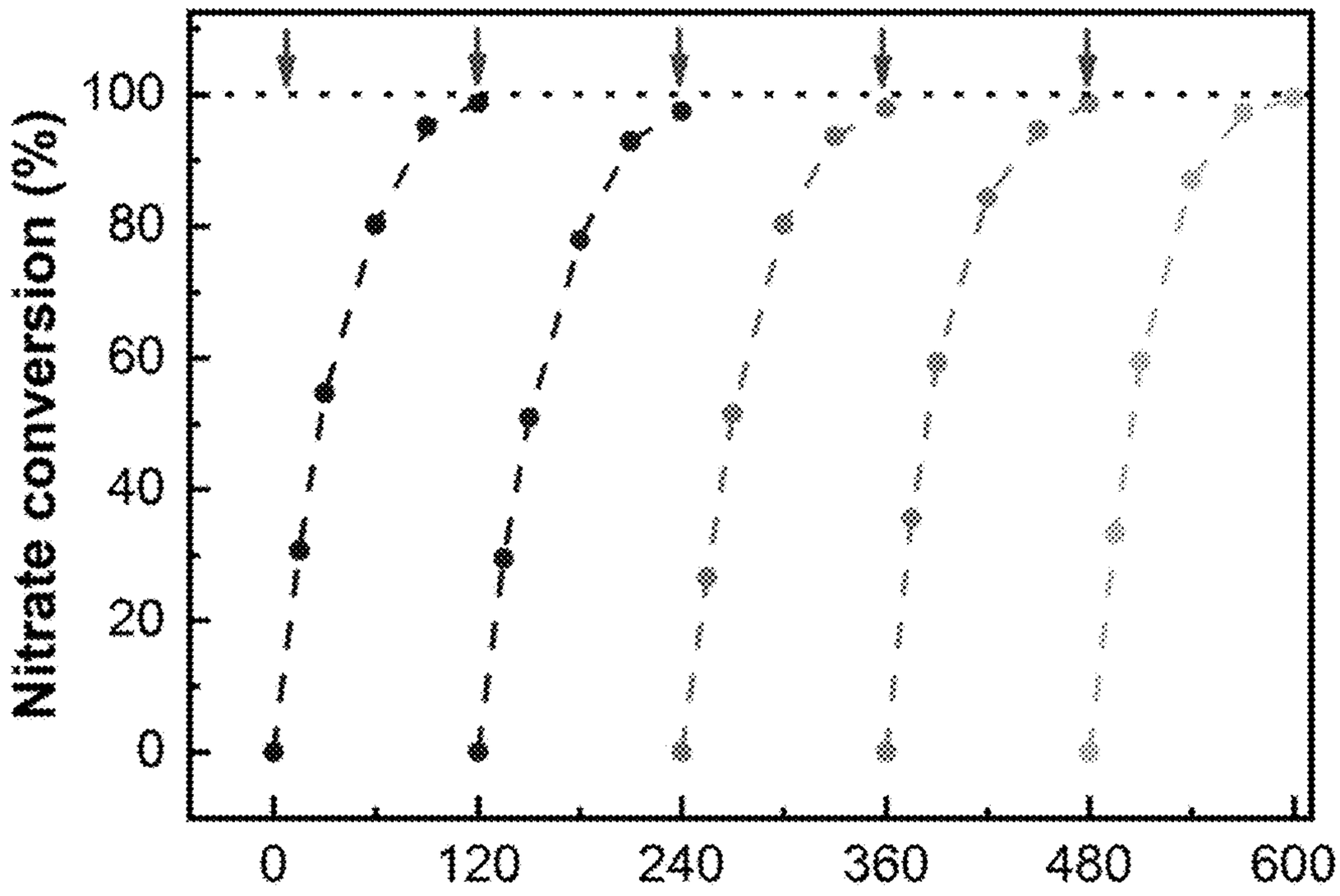
Nitrate conversion (%)
100
80
60
40
20
0
0
120
240
360
480
600
Time (min)

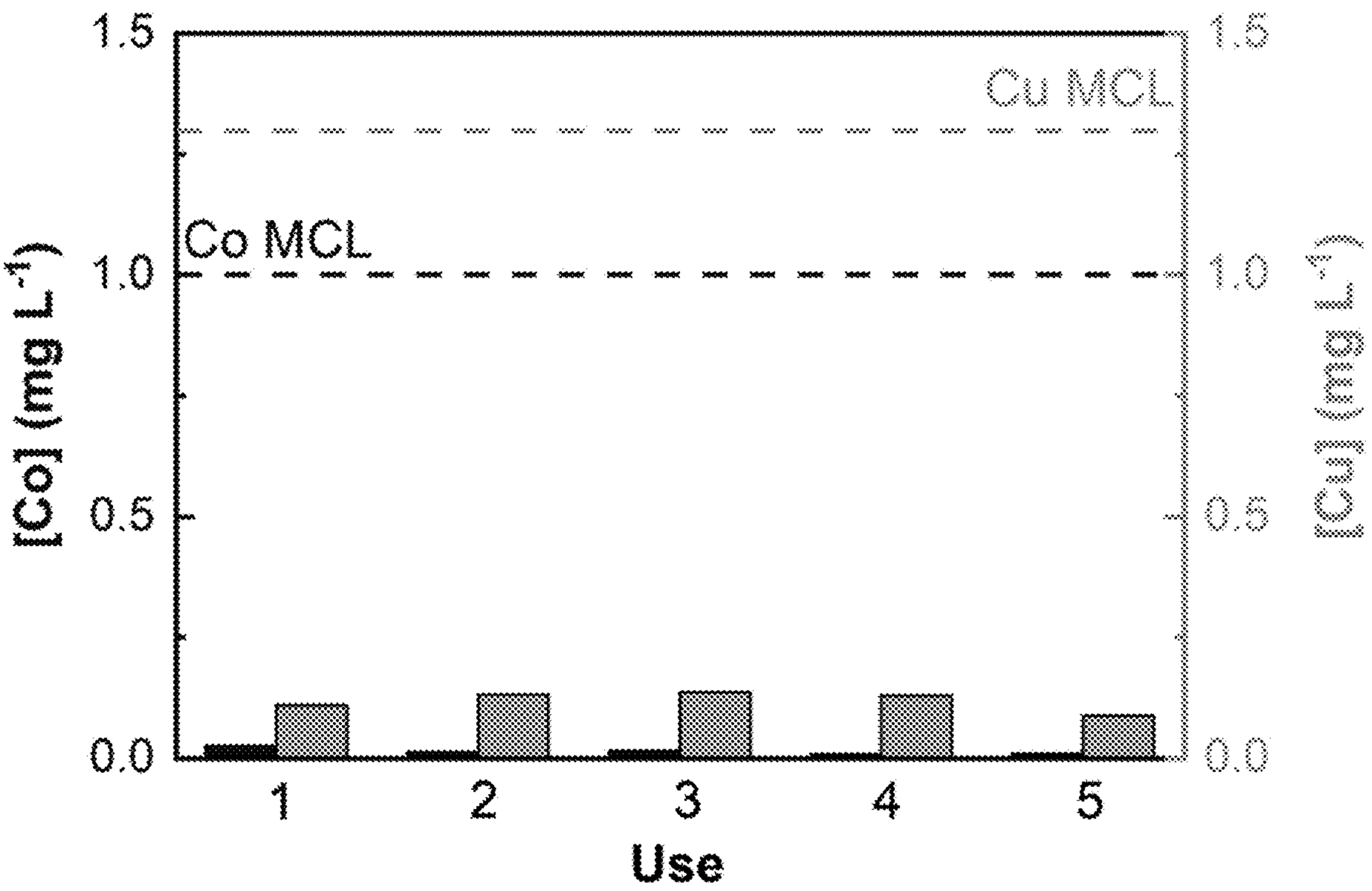
[Co] (mg L-1)
[Cu] (mg L-1)
1.5
1.0
0.5
0.0
Co MCL
Cu MCL
1
2
3
4
5
Use

FIG. 6B

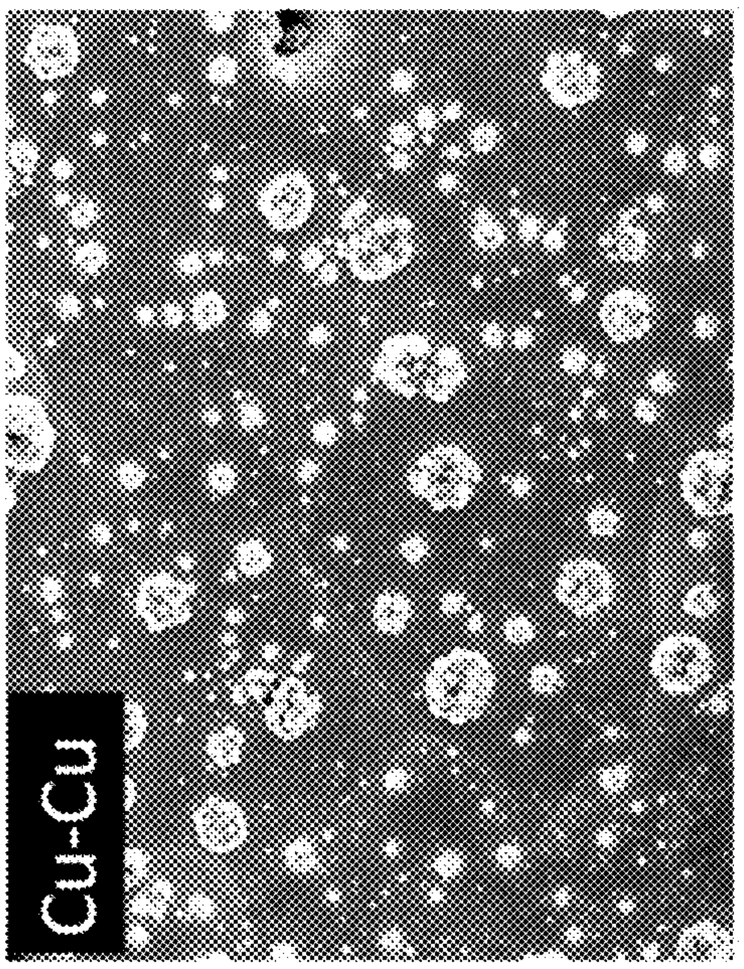

FIG. 7B

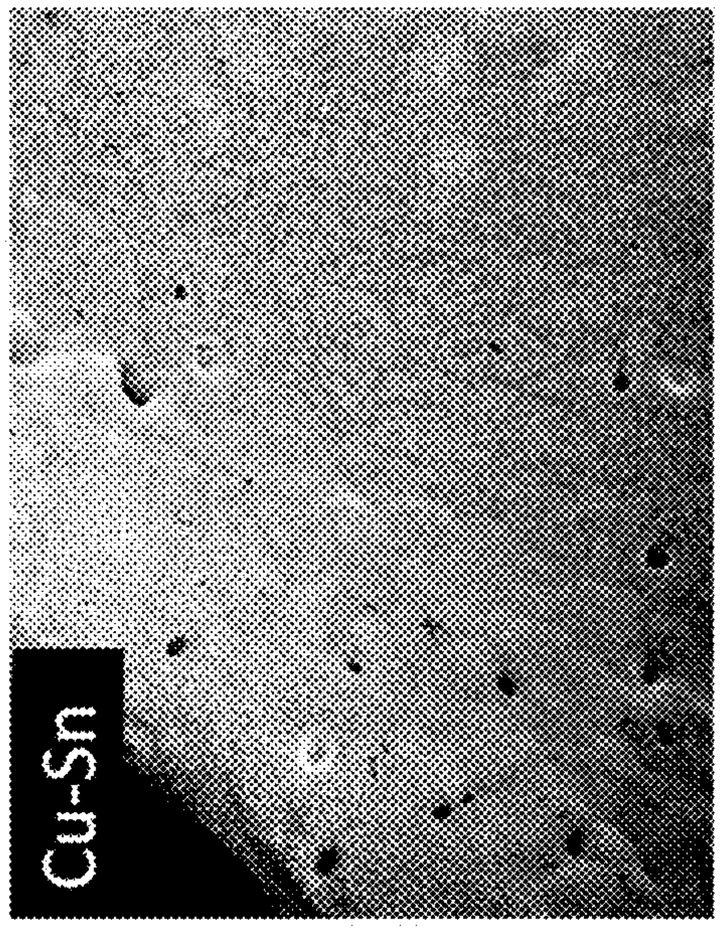

FIG. 7D

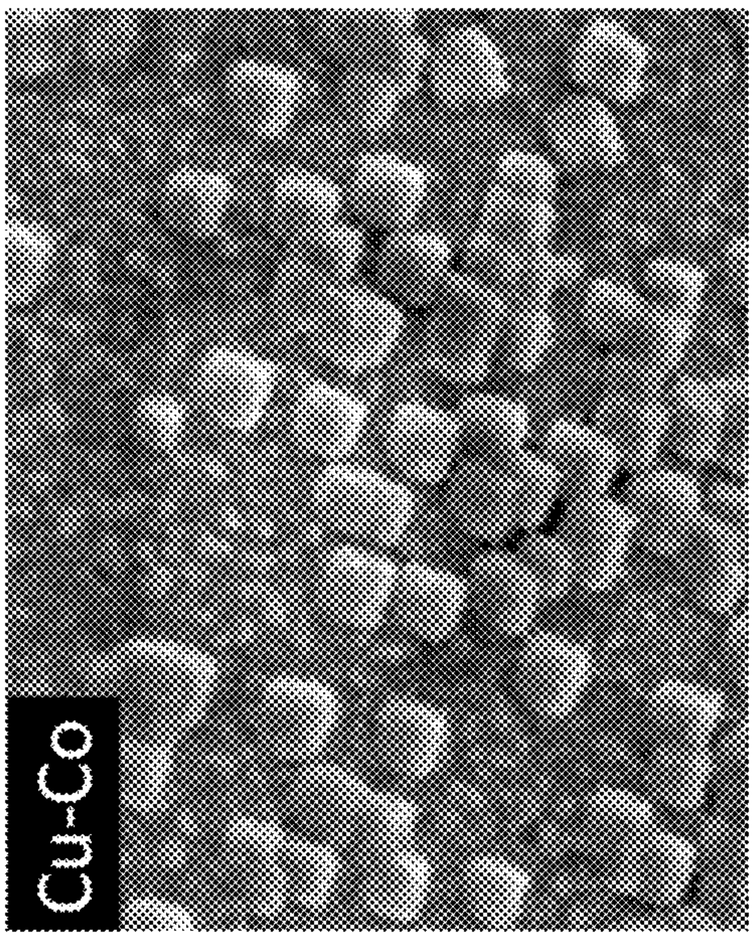

FIG. 7A

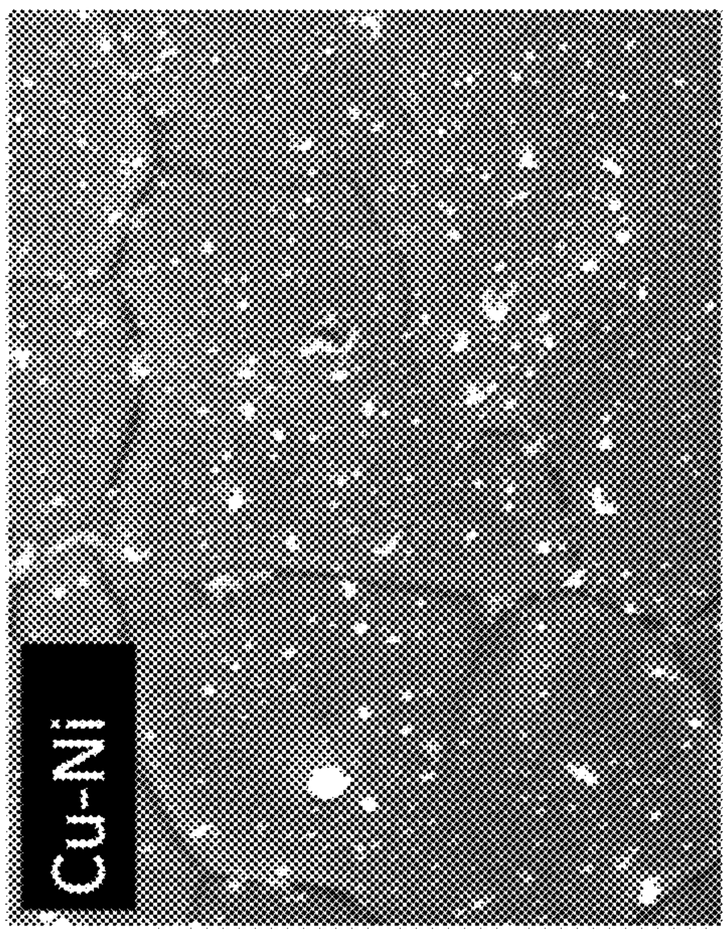

FIG. 7C

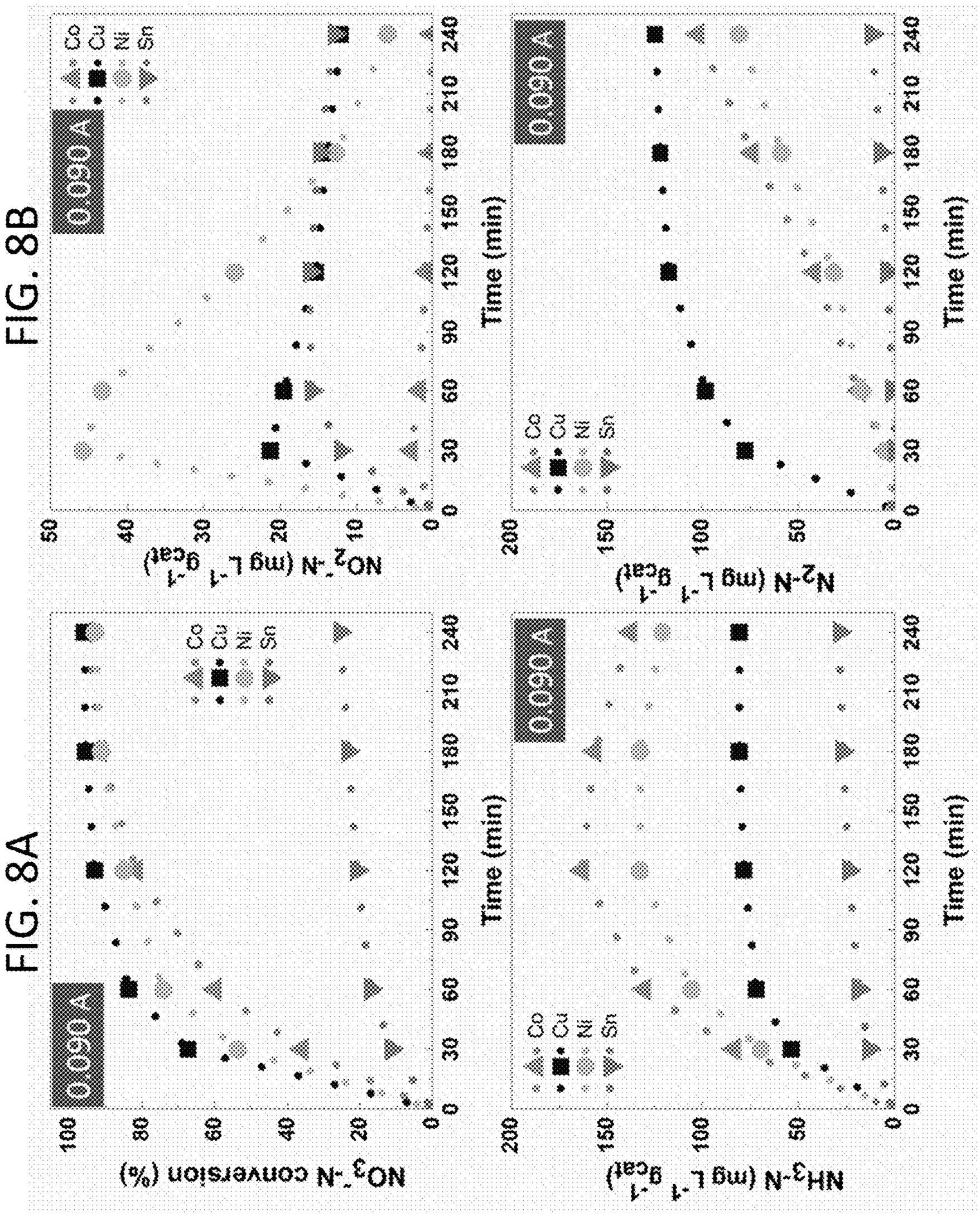

FIG. 8A

FIG. 8B

FIG. 8C

FIG. 8D

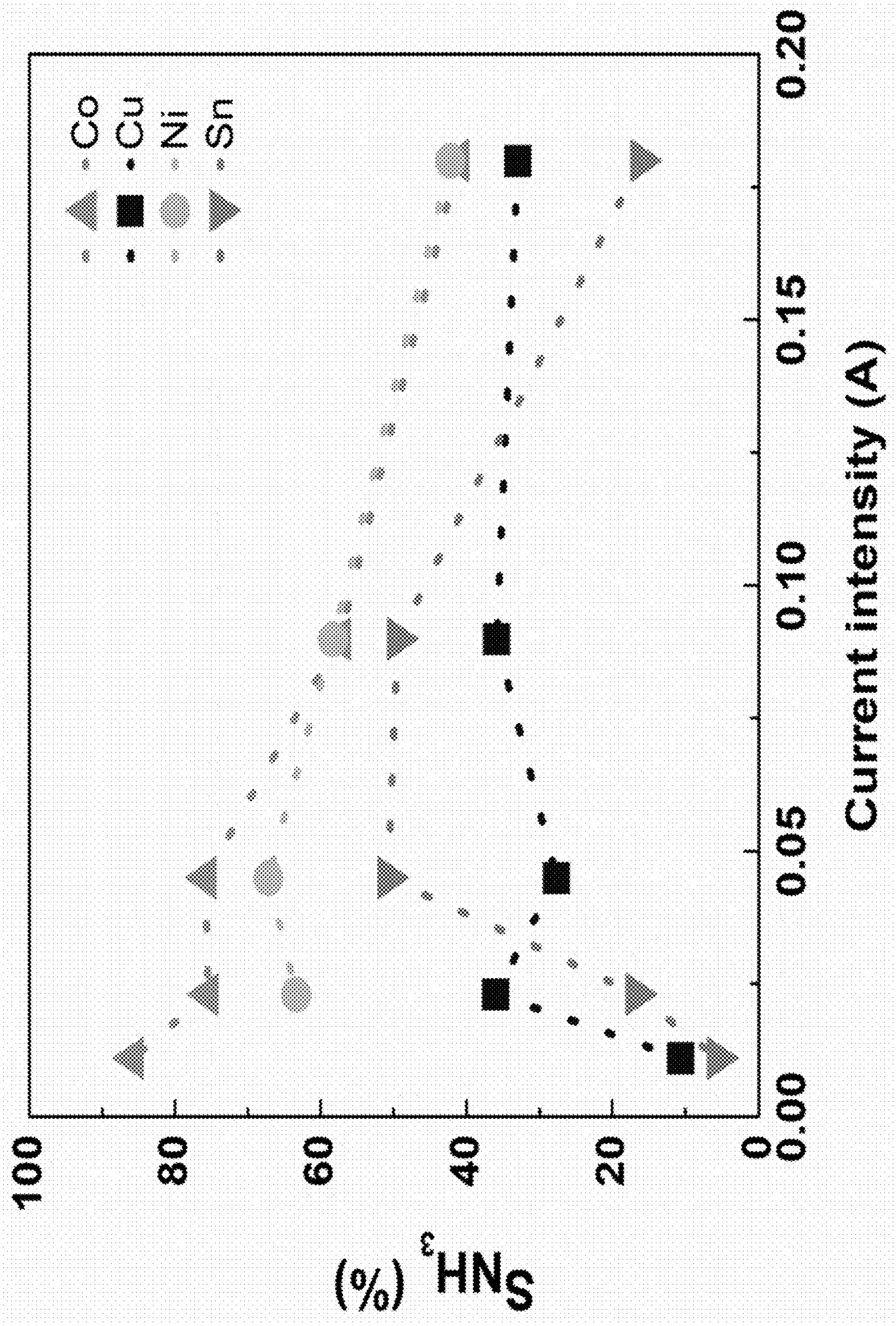
Co
Cu
Ni
Sn
0.20
0.15
0.10
0.05
0.00
Current intensity (A)
100
80
60
40
20
0
S_3N_H (%)

FIG. 9

COBALT-COPPER NANOENABLED ELECTRODES

CROSS-REFERENCE TO RELATED APPLICATION

[0001] This application claims the benefit of U.S. Patent Application No. 63/344,749, filed on May 23, 2022, which is incorporated herein by reference in its entirety.

STATEMENT OF GOVERNMENT SUPPORT

[0002] This invention was made with government support under 1449500 awarded by National Science Foundation. The government has certain rights in the invention.

TECHNICAL FIELD

[0003] This invention relates to cobalt-copper bimetallic three-dimensional electrodes, methods of fabricating the electrodes, and use of the electrodes (e.g., for electrocatalytic reduction of nitrate to ammonia).

BACKGROUND

[0004] Ammonia is a major component in most crop fertilizer formulations. Despite the benefits of ammonia production, indirect hazardous effects related to ammonia usage causes serious environmental problems related to the anthropogenic disruption of the natural nitrogen cycle. Ammonia leaches into ground and surface waters is easily transformed in the environment via biotic and abiotic processes to nitrate. Nitrate pollution in waters is due to anthropogenic activities including but not limited to fertilizer runoff from crops, animal farming, and industrial wastewater.

SUMMARY

[0005] The disclosure relates to cobalt nanocomposites electrodeposited over copper foams to yield cobalt-copper nanoenabled electrodes, methods of fabricating the electrodes, and use of the electrodes (e.g., for the electrocatalytic reduction of nitrate to ammonia). These Cu/Co_3O_4 and/or $Cu/Co(OH)_x$ foam electrodes facilitate electrochemical reduction of nitrate (ERN) by introducing bimetallic active catalytic sites which produce a higher nitrate conversion when compared to the pristine Cu electrode, due at least in part to the synergistic interactions between Cu and Co. The Cu surface catalyzes the reduction of nitrate to nitrite, while the Co sites increase the conversion of nitrite to ammonia. Faradaic efficiency of the Cu/Co_3O_4 and/or $Cu/Co(OH)_x$ electrode is at least two-fold higher with an energy consumption four-times lower than monometallic Cu foam. The bimetallic electrocatalysts perform better and produce a greater yield than pure platinum group metal (PGM) catalysts and bimetallic Cu/Pt electrodes.

[0006] In a first general aspect, a nanocomposite electrode includes a porous copper substrate and Co_3O_4 and/or $Cu/Co(OH)_x$ nanoparticles electrolytically deposited on the porous copper substrate.

[0007] Implementations of the first general aspect include one or more of the following features.

[0008] An average size of the Co_3O_4 and/or $Cu/Co(OH)_x$ nanoparticles is typically in a range of 50 nm to 500 nm. In some cases the porous copper substrate is a copper foam. The porosity of the copper foam can be in a range of 5 to 200 pores per inch. The Co_3O_4 and/or $Cu/Co(OH)_x$ nanoparticles extend from pore surfaces of the porous copper substrate, are bound to the porous copper substrate, or both. A volume of the nanocomposite electrode is at least 0.1 cm^3.

[0009] In a second general aspect, making a nanocomposite electrode includes contacting a porous copper substrate with a solution comprising cobalt, and electrodepositing the cobalt on the porous copper substrate to yield the nanocomposite electrode.

[0010] Implementations of the second general aspect include one or more of the following features.

[0011] In one example, the porous copper substrate is a copper foam. The solution typically includes a cobalt salt in a range of 0.1 mol to 5 mol L^{-1}, boric acid in a range of 0.1 mol L^{-1} to 5 mol L^{-1}, sodium sulfate in a range of 0.01 mol L^{-1} to 1.0 mol L^{-1}, or any combination thereof. Electrodepositing the cobalt on the porous copper substrate includes forming Co_3O_4 and/or $Cu/Co(OH)_x$ nanoparticles on surfaces of the porous copper substrate. An average size of the Co_3O_4 and/or $Cu/Co(OH)_x$ nanoparticles is typically in a range of 50 nm to 500 nm.

[0012] In a third general aspect, reducing nitrate to ammonia includes contacting the nanocomposite electrode of the first general aspect with an aqueous solution comprising nitrate, and electrocatalytically reducing the nitrate to yield ammonia.

[0013] Implementations of the third general aspect include one or more of the following features.

[0014] Some implementations include electrocatalytically reducing the nitrate to yield nitrite, and electrocatalytically reducing the nitrite to yield ammonia. Electrocatalytically reducing the nitrate to yield nitrite is facilitated by copper in the porous copper substrate. Electrocatalytically reducing the nitrite to yield ammonia is facilitated by cobalt in the cobalt nanoparticles.

[0015] The bimetallic Cu/Co_3O_4 and/or $Cu/Co(OH)_x$ electrodes referred as Cu/Co can be used for the conversion of a common contaminant in water sources (nitrate) to produce an agricultural commodity (ammonia), enabling decentralized ammonia recovery from polluted water sources. The electrodes do not rely on PGM materials, but rather use cheaper and more abundant materials as electrocatalysts. The electrodeposition method provides a stronger physical attachment between material interfaces than drop casting. The method can generate stable Cu/Co nanoenabled electrodes for sustained performance of nitrogen management electrified systems.

[0016] The details of one or more embodiments of the subject matter of this disclosure are set forth in the accompanying drawings and the description. Other features, aspects, and advantages of the subject matter will become apparent from the description, the drawings, and the claims.

BRIEF DESCRIPTION OF DRAWINGS

[0017] FIGS. **1**A and **1**B depict metal electrodeposition and nitrate reduction as described herein.

[0018] FIGS. **2**A and **2**B show linear sweep voltammetry at 10 mV s^{-1} of Cu foam and Cu/Co structure in different solution of 0.1 mol L^{-1} Na_2SO_4 with 20 mmol L^{-1} $NaNO_2$ (FIG. **2**A) and 20 mmol L^{-1} $NaNO_3$ (FIG. **2**B).

[0019] FIGS. **3**A and **3**B show time-course of N-species (mg L^{-1}) for electrolysis of 30 mg NO_3^-—N L^{-1} at 20 mA cm^{-2} using Cu foam and Cu/Co, respectively

[0020] FIGS. **4**A and **4**B show concentration of N-species over time for the electrolysis of 30 mg NO_2^-—N L^{-1} using Cu foam and Cu/Co, respectively, at 20 mA cm^{-2} (including kinetic constant of NO_2^- reduction in a pseudo-first order reaction).

[0021] FIG. **5**A shows kinetic constant and electrical energy per order for ammonia production using Cu foam, Cu/Pt and Cu/Co electrodes. FIG. **5**B shows ammonia yield and Faradaic efficiency after 120 min of electrolysis using Cu foam, Cu/Pt and Cu/Co electrodes. Including percentage of ammonia conversion from initial N-content.

[0022] FIG. **6**A shows nitrate conversion percentage during 5 cycles; arrows indicate solution renewal. FIG. **6**B shows copper and cobalt concentration in solution after 5 cycles. Maximum concentration level for each element is shown in dashed lines.

[0023] FIGS. **7**A-**7**D are scanning electron microscope (SEM) images of different bimetallic electrodes.

[0024] FIGS. **8**A-**8**D show electrochemical reduction of nitrate with the evolution of nitrate, ammonia, and nitrogen gas.

[0025] FIG. **9** shows selectivity toward ammonia from the electrochemical reduction of nitrate at different current intensities.

DETAILED DESCRIPTION

[0026] This disclosure relates to cobalt nanocomposites electrodeposited over copper foams to yield Cu/Co nanoenabled electrodes, methods of fabricating the electrodes, and use of the electrodes. The electrodes are suitable for the electrocatalytic reduction of nitrate to ammonia as shown in Eq. 1.

$$NO_3^- + 9H^+ + 8e^- \rightarrow NH_3 + 3H_2O \quad (1)$$

These Cu/Co foam electrodes facilitate electrochemical reduction of nitrate (ERN) by introducing bimetallic active catalytic sites which produce a higher nitrate conversion when compared to the pristine Cu electrode, due at least in part to the synergistic interactions between copper and cobalt. The Cu surface catalyzes the reduction of nitrate to nitrite, while the Co nanoparticles increase the conversion of nitrite to ammonia. In one example, Faradaic efficiency for Cu/Co was two-fold higher with an energy consumption four-times lower than pristine Cu foam. The bimetallic Cu/Co electrocatalysts showed higher performance and yield than Cu/Pt electrodes, while not relying on platinum-group materials.

[0027] FIG. **1**A depicts cobalt electrodeposition on a porous copper substrate to yield a nanocomposite electrode. The nanocomposite electrode includes a porous copper substrate, and Co_3O_4 and/or $Cu/Co(OH)_x$ nanoparticles (referred as Co nanoparticles) electrolytically deposited on the porous copper substrate. An average size of the Co nanoparticles is in a range of 50 nm to 500 nm. The porous copper substrate can be a copper foam. A porosity of the copper foam is typically in a range of 5 to 200 pores per inch. The Co nanoparticles are bound to the porous copper substrate and can extend from pore surfaces of the porous copper substrate. A volume of the nanocomposite electrode is at least 0.1 cm^3.

[0028] Fabricating the nanocomposite electrode includes contacting a porous copper substrate with a solution comprising cobalt, and electrodepositing the cobalt on the porous copper substrate to yield the nanocomposite electrode. The porous copper substrate can be a copper foam. The solution typically includes a cobalt salt in a range of 0.1 mol L^{-1} to 5 mol L^{-1}. In some cases, the solution comprises boric acid in a range of 0.1 mol L^{-1} to 5 mol L^{-1}, sodium sulfate in a range of 0.01 mol L^{-1} to 1.0 mol L^{-1}, or both. Electrodepositing the cobalt composites on the porous copper substrate includes forming Co_3O_4 and/or $Cu/Co(OH)_x$ nanoparticles on surfaces of the porous copper substrate. An average size of the Co nanoparticles is in a range of 50 nm to 500 nm.

[0029] Reducing nitrate to ammonia includes contacting a nanocomposite electrode as described herein with an aqueous solution comprising nitrate, and electrocatalytically reducing the nitrate to yield ammonia. The nitrate can be electrocatalytically reduced to yield nitrite, and the nitrite can be electrocatalytically reduced to yield ammonia. Electrocatalytically reducing the nitrate to yield nitrite is facilitated by copper in the porous copper substrate, and electrocatalytically reducing the nitrite to yield ammonia is facilitated by cobalt in the cobalt nanoparticles.

Examples

Chemicals and Materials

[0030] Ultrapure water was used for all solutions with resistivity >18.2 MΩ cm at 25° C. provided by Elga Water. Sodium sulfate (Na_2SO_4) purchased from Sigma-Aldrich was used as supporting electrolyte. The different solutions containing nitrogen inorganic species supplied by Sigma-Aldrich were prepared with analytical grade sodium nitrate ($NaNO_3$), sodium nitrite ($NaNO_2$), and/or ammonium sulfate ($(NH_4)_2SO_4$). Copper foam (110 pores per inches, 4.5 cm^2, 2 mm thick) with 99.99% purity was purchased from Futt and used as the three-dimensional electrode. Electrodes were nanoenabled with cobalt by using ($CoSO_4 \cdot 6H_2O$) and boric acid (H_3BO_3) acquired from Sigma-Aldrich. Acetone ($(CH_3)_2CO$) and hydrochloric acid (HCl), provided by Sigma-Aldrich, were used for copper surface pretreatment.

Electrodeposition of Co Nanocomposites Over Cu Substrate

[0031] The electrodeposition of Co nanocomposites over Cu foam electrodes was performed by chronoamperometry using a PGSTAT302N-Metrohm potentiostat. To remove surface impurities, Cu foams were pretreated by sonicating them in acetone for 15 min to remove organic compounds and greases, placed in 0.1 mol L^{-1} HCl for 5 min, thoroughly rinsed with ultrapure water, and dried with a heat gun at 50° C. The electrodeposition was conducted in a three-electrode cell using Ag/AgCl (3.5 M KCl) as the reference electrode, platinum plate as the counter-electrode, and Cu foam as the working electrode. The electrodeposition bath consisted of 0.5 mol L^{-1} $Co(SO_4)_2 \cdot 6H_2O$, 0.5 mol L^{-1} H_3BO_3, and 0.1 mol L^{-1} Na_2SO_4 with a final pH of 4.5. The working electrode was submitted to cathodic polarization conditions at −1.2 V vs Ag/AgCl during 180 s. Thereafter the electrodes were dried using a heat gun at 50° C. and the electrode mass was registered.

Characterization of Three-Dimensional Electrodes

[0032] X-ray photoelectron spectroscopy (XPS) was employed to study the element valence state on the surface using a VG 220i-XL instrument equipped with a monochromic Al K_α X-ray source with a line width of 0.7 eV. The

morphology and elemental analysis were carried out by scanning electron microscope coupled with energy-dispersive X-ray spectroscopy (SEM-EDS) using an Auriga FIB-SEM provided by Zeiss under 10 kV, 5 nA and 5.0 WD for SEM images.

[0033] The electrochemical characterization was carried out by linear sweep voltammetry (LSV) in a conventional three-electrode system. The three-electrode system was set up using Cu foam (nanomodified or pristine) as the working electrode, Ag/AgCl (3.5 mol L^{-1} KCl) as the reference electrode, and Pt coil as the counter electrode. Geometrical area (cm^2) was considered to define current density. Solutions were deaerated with N_2 before carrying out electrochemical measurements to ensure the absence of oxygen dissolved in the electrolyte. The electrochemical behavior and direct electron transfer for ERN of each electrode were tested by linear sweep voltammetry (LSV). LSV was performed at 10 mV s^{-1} in solutions of 0.1 mol L^{-1} Na_2SO_4 as support electrolyte, in presence or absence of 20 mmol L^{-1} nitrogen oxyanions (i.e., $NaNO_3$ or $NaNO_2$) to assign reduction peaks.

Electrochemical Reduction of Nitrate

[0034] The electrocatalytic reduction of nitrate was carried out in a batch reactor at 25° C. using 100 mL of non-deaerated 30 mg L^{-1} NO_3^-—N solution with 12.5 mmol L^{-1} Na_2SO_4. Electrolysis was conducted under magnetic stirring at 500 rpm to ensure transport from/towards the electrode surface. The initial pH and conductivity conditions were 5.90±0.2 and 3.20±0.05 mS cm^{-1}, respectively. All tests were operated under galvanostatic conditions using a power supply (TENMA 72-2720 DC) at 20 mA cm^2. The Cu and Cu-nano enabled foams were used as cathodes and commercial Ti/IrO_2 (DeNora—USA) as anode in a two-electrode system. Blank tests were measured using 30 mg L^{-1} NO_2^-—N or 30 mg L^{-1} NH_3—N in 12.5 mmol L^{-1} Na_2SO_4. Aliquots of ~2.0 mL were withdrawn as samples at specific electrolysis times during the 120 min of treatment time to analyze NO_3^-—N, NO_2^-—N, and NH_3—N. All the ERN tests were performed in triplicate and deviations between them were lower than 5% for all trials.

Analytical Instruments and Performance Evaluation

[0035] Thermo Scientific Orion Star A221 meters were used to assess the pH and conductivity. Nitrate (mg NO_3^-—N L^{-1}), nitrite (mg NO_2^-—N L^{-1}), and ammonia (mg NH_3—N L^{-1}) concentrations were followed over time using TNT 835, TNT 839 and TNT 830 HACH kits, respectively, which were measured in a HACH DR6000 UV-vis equipment. The nitrate conversion was calculated using Eq. 2,

$$\text{Nitrate conversion}(\%) = \frac{C_{nitrate,i} - C_{nitrate,t}}{C_{nitrate,i}} \times 100 \tag{2}$$

where $C_{nitrate,i}$ is the nitrate concentration in mg NO_3^-—N L^{-1} before treatment, and $C_{nitrate,t}$ is the nitrate concentration at time (t). N-volatile species (N_2, NO, NO_2 or N_2O) were determined by mass balance on aqueous nitrogen species and labeled as N-gas.

[0036] Faradaic efficiency (FE) estimated from Eq. 3 was used as a figure of merit to determines system performance from the number of electrons consumed in an electrochemical reaction relative to the expected theoretical conversion ruled by Faraday's law:

$$FE = \frac{n\ F\ N_i}{3600\ I\ t} \times 100 \tag{3}$$

where n is the number of electrons required per mol of ammonia (mol), F is the Faraday constant (96 487 C mol^{-1}), N_i is the mol of ammonia generated during the electrolysis, I is the applied electric current (A), t is the electrolysis time (h), and 3600 is a unit conversion factor (3600 s h^{-1}).

[0037] Electrical energy per order (EE/O) was used as an engineering figure of merit to benchmark the electric energy required to reduce NO_3^-—N concentration by one order of magnitude in a unit volume calculated from Eq. 4 for batch operation mode,

$$EE/O\ (\text{kWh}\ m^{-3}\text{order}^{-1}) = \frac{E_{cell} I t}{V_3 \log(C_0/C_t)} \tag{4}$$

where E_{cell} is the average of the cell potential (V), I is current intensity (A), t is time (h), V_s is solution volume (L), and C_0 and C_t are the initial and final concentration after one order of magnitude reduction of nitrate.

Physical Characterization of Three-Dimensional Copper Foam Nanoenabled with Cobalt

[0038] The chemical composition of Cu foam was evaluated before and after electrodeposition of cobalt-based nanostructures by a wide-range XPS. Pristine Cu foam showed a defined Cu 2p peak signal and the characteristic peaks of C 1s, O 1s due to presence of atmospheric carbon molecules and metal oxide present on the surface, respectively, whereas the XPS spectrum of Co-enabled Cu foam presented only a Co 2p signal beyond the C 1s, O 1s peaks. The absence of Cu 2p peaks in the wide-range spectra after electrodeposition suggested an effective superficial coverage of Cu foam surface since XPS is surface sensitive. The high-resolution XPS for Cu 2p in Cu foam demonstrated the co-existence of Cu^0, Cu^{1+}, and Cu^{2+}, which confirms the co-existence of pure copper with superficial copper oxide. The difference between Cu^0 and Cu^{1+} is difficult to discern due to small binding energy shift (~0.3 eV) between both species. Thus, the deconvolution of the Cu $2p_{3/2}$ spectrum involved mainly two peaks at 930.9 eV and 932.6 eV that correspond to Cu^0/Cu^{1+} and Cu^{2+}, respectively. The Cu $2p_{1/2}$ spectrum showed peaks at 950.8 eV and 952.4 eV, related to Cu^0/Cu^{1+} and Cu^{2+}, respectively. The absence of well-defined Cu peaks in the high-resolution spectra for Cu 2p in Cu/Co_3O_4 can be explained by the wide coverage of the substrate with Co composites. The Co 2p high-resolution XPS spectrum revealed the presence of both species Co^{2+} and Co^{3+}. In Co $2p_{3/2}$ the peaks at 779.2 eV and 781.6 eV were related to Co^{3+} and Co^{2+}, respectively. The peak of Co $2p_{1/2}$ was separated into two peaks for Co^{2+} at 796.2 eV and Co^{3+} at 798.5 eV. This result suggests that the cobalt generated on the surface is mostly a mixed oxide of cobalt. The O 1s spectrum was associated with the nanoenabled Cu/Co_3O_4 was deconvoluted into three peaks. The first peak at 530.5 eV (O1) was related to the OH^- group from cobalt hydroxides on the surface. The second peak was centered at 531.8 eV (O2) and can be attributed to oxygen vacancy in

the structure, such as Co_3O_4 structures that enable formation of a higher oxidation state of cobalt (i.e., Co^{3+}) or mixed hydroxides of $Co(OH)_3$ and $Co(OH)_2$ referred as $Co(OH)_x$. The third peak related to chemisorbed oxygen (O3) was observed at 532.6 eV. The pristine Cu foam high-resolution spectra of O 1s showed the same three peaks of oxygen species but with one order of magnitude lower intensity, suggesting a lower content of oxygen on the surface. The increase on O 1s intensity is therefore associated with the surface coverage with cobalt oxide structures. The XPS analysis provides evidence for the formation of cobalt oxide structures during electrodeposition and against the formation of metallic cobalt domains at the electrode interface.

[0039] Morphological characterization of the pristine Cu foam and the Cu/Conanocomposites was performed by field-emission scanning electron microscope (FE-SEM). Results show that the morphology of the Cu foam is a porous three-dimensional arrangement. Additionally, at a higher magnification (80,000×), the pristine Cu foam appeared as a smooth surface without any composites. Conversely, the Cu/Co electrode shows nanoflake shaped composites over the Cu surface with an average size around 70 nm. An enlarged image revealed the porous surface formed by the Co_3O_4 and/or $Cu/Co(OH)_x$ nanoflakes on the surface. This micrography illustrates the wide coverage of Co structures on the electrode surface in agreement with the XPS results discussed above. The energy-disperse X-ray spectroscopy (EDS) mapping displayed the elemental composition of Cu, Co, and O on the surface of the Cu/Co electrode. The increase of oxygen element in comparison with the Cu foam EDS shown in Table 1 represents the oxide compound in the surface after the electrodeposition. The higher oxygen coverage observed in the Cu/Co EDS was in agreement with the XPS results that showed an order of magnitude higher intensity for the Cu/Co when compared with pristine Cu.

TABLE 1

Elemental composition calculated from EDS analysis for Cu foam and Cu/Co electrodes.

	Composition (wt %)	
Element	Cu foam	Cu—Co_3O_4
Cu	98.55	82.71
O	1.45	6.80
Co	—	10.49

Analysis of the Cu/Co Electrochemical Nitrate Reduction

[0040] Electrochemically driven resource recovery approaches from nitrate polluted wastewater aim to recover selectively ammonia as a final product. The reduction reaction of nitrate initially generates nitrite as intermediate stable species following reaction (5). Subsequent reduction leads to the formation of ammonia according to reaction (6).

$$NO_3^- + 2H^+ + 2e^- \rightarrow NO_2^- + H_2O \quad (5)$$

$$NO_2^- + 7H^+ + 6e^- \rightarrow NH_3 + 2H_2O \quad (6)$$

[0041] To analyze the charge transfer processes involved at the different electrocatalytic interfaces, linear sweep voltammetry (LSV) of a 20 mmol L^{-1} NO_2^- was evaluated first to identify the thermodynamic conditions of Eq. 6 that yield ammonia from nitrite. FIG. **1**A shows LSV plots for pristine and Co-nanoenabled electrodes. An increase on the current density response was registered when comparing a blank solution of inert electrolyte Na_2SO_4 against a solution containing the electroactive target species nitrite. The LSV in presence of NO_2 depicts a shoulder overlapped with the current associated to hydrogen gas evolution with an onset potential at −1.2 V vs Ag/AgCl. The comparison between blank and nitrite containing solution suggests that nitrite reduction (Eq. 6) and hydrogen evolution reaction (Eq. 10) are competitive processes coexisting under cathodic polarization conditions at the potential range required for ammonia production. While no major differences on current response were observed for LSV of blank solutions using either Cu foam or Cu/Co electrode, there is a difference of over 15 mA cm^{-2} at a given potential when comparing both materials LSV response in presence of 20 mM NO_2^-. The increase in current density response suggests a higher electrocatalytic response and an enhanced charge transfer reaction at the nanocomposite electrode interface.

[0042] The LSV of nitrate solutions in FIG. **1**B show two resolved shoulders overlapped with hydrogen evolution. The previous analyses conducted with nitrite allows clear assignment of each reduction peak to a specific overall reduction process. The first peak ca. −1.0 V vs Ag/AgCl can be assigned to NO_3^- reduction to NO_2^-; whereas the following peak (also observed in FIG. **3***a*) at more negative potential of −1.4 V vs Ag/AgCl correspond to the subsequent reduction from NO_2^- to NH_3. Analysis of by-products yielded from potentiostatic reductions at these defined potentials confirm that the main by-products formed are nitrite at −1.0 V vs Ag/AgCl and ammonia at −1.4 V vs Ag/AgCl.

[0043] The higher current density registered for Cu/Co electrodes can be related to the involvement of adsorbed hydrogen. Cobalt-based structures present high affinity for hydrogen dissociative adsorption during water splitting yielding highly reductive monoatomic $H_{(ads)}$. The involvement of hydrogenation simultaneously occurring along with direct charge transfer processes is a fundamental synergistic process still unconfirmed for nitrate reduction. The hydrogenation contribution to overall oxyanion reduction can be one of the reasons for the higher performance of noble metals such as Pt or Pd. One intermediate formed during the chemical and electrochemical reactions involved in nitrate reduction is adsorbed *NO. The adsorbed *NO species are susceptible to react with adsorbed $H_{(ads)}$ on the electrode surface and steer the product selectivity towards ammonia through reaction (7) or nitrogen gas through reaction (8) depending on the N/H coverage ratio, respectively.

$$*NO + 5H_{(ads)} \rightarrow *NH_3 + H_2O \quad (7)$$

$$2*NO + 4H_{(ads)} \rightarrow *N_2 + 2H_2O \quad (8)$$

[0044] Hydrogen evolution reaction (HER) can be considered an elemental process for enabling simultaneous catalytic hydrogenation (depending on the nature of the catalyst) as well as a competitive reaction. The electrochemical production of stable adsorbed elemental hydrogen (H_{ads}, Eq. 9) can yield either to the recombination evolving H_2 from Eq. 10 or drive the selective control on reduction products according to chemically driven Eq. (7) and/or (8).

$$H_2O + e^- \rightarrow H_{(ads)} + OH^- \quad (9)$$

$$H_{(ads)} + H_{(ads)} \rightarrow H_{2(g)} \quad (10)$$

Analysis of the Electrochemical Reduction of Nitrate Using Cu/Co Electrodes

[0045] Electrochemical reduction of nitrate was conducted under comparable conditions to benchmark performance of pristine Cu foam and Cu/Co catalytic materials. The time-course of N-species (mg-N L^{-1}) during electrocatalytic treatment is shown in FIGS. **2**A and **2**B. Gradual conversion of nitrate (NO_3^-) to nitrite (NO_2^-), ammonia (NH_3), and nitrogen gas species (N gas) occurs for both materials but at different rate and selectivity. After 120 min, almost complete nitrate conversion (ca. 98.5%) was attained by Cu/Co cathodic electrocatalyst ($k_1=5.9\times10^{-4}$ s^{-1}, $R^2=0.997$), while the Cu foam solely led to 82.5% ($k_1=1.3\times10^{-4}$ s^{-1}, $R^2=0.988$). The Cu foam reached the highest amount of NO_2 accumulated of 6.19 mg-N L^{-1} after 60 min, which decreased thereafter down to 4.36 mg-N L^{-1} at the end of the treatment. Conversely the Cu/Co nanocomposites reached a lower maximum NO_2^- concentration of 1.61 mg-N L^{-1} after 15 min of treatment, which dropped down to 0.41 mg-N L^{-1} (below the nitrite MCL of 1.0 mg-N L^{-1}) after 60 min of treatment and became completely negligible later. These results are in in agreement with the higher electrocatalytic activity of Cu/Co nanocomposite electrodes for nitrate and nitrite reduction observed during electroanalytical characterization of electrodes. The enhanced reduction performance induced by cobalt sites explains the lower accumulation of nitrite that is readily reduced after generation from reaction (6).

[0046] Product selectivity is a factor in the recovery of N-sources as ammonia. While Cu foam allowed obtaining up to 18.9 mg-N L^{-1} after 120 min, the Cu/Co attained 26.3 mg-N L^{-1} at 90 min, which is 1.4 times higher concentration. The decrease in ammonia concentration in solution after 90 min electrolysis with Cu/Co down to 24.0 mg-N L^{-1} at 120 min may be related to volatiles stripping induced by the high alkaline pH. This effect can be explained by the promotion of NH_3 gas formation since its acid dissociation constant ($K_a=10^{-9.3}$ or $pKa_{NH3}=9.3$) is lower than final pH (~11.0). Regarding the nitrogen mass balance, about 1.5 mg-N L^{-1} and 5.56 mg-N L^{-1} left the solution in gas phase, at the end of the treatment time, for the Cu foam and Cu/Co, respectively.

[0047] To better understand the reasons related to the low accumulation of nitrite when comparing Cu/Co with pristine Cu, electrochemical reduction of nitrite solutions was studied. FIGS. **3**A and **3**B compares the time course of N-species during the reduction of 30 mg-N L^{-1} of NO_2^- over 120 min. The NO_2^- constant kinetic decays (k_1) fitted well a pseudo-first order reaction. When using the Cu/Co material as cathode, k_1 was 2 times higher ($k_1=1.2\times10^{-3}$ s^{-1}) than the value obtained with Cu foam ($k_1=0.6\times10^{-3}$ s^{-1}). In fact, the nanocomposite Cu/Co completely reduced nitrite in 60 min, while bare Cu required the double of the time. Regardless the cathodic material used, NH_3 was the preferential product obtained from NO_2^- reduction with similar maximum concentration after 60 min of treatment, $[NH_3]_{Cu\ foam}=25.5$ mg-N L^{-1} and $[NH_3]_{Cu/Co}=27.6$ mg-N L^{-1}. These results demonstrated the catalytic effect of Co sites that accelerate nitrite reduction for ammonia production. The Co sites can provide the capability to increase the amount of Haas in the electrode surface to reduce NO (Eq. 7). Nitrite is a readily reducible species through catalytic hydrogenation while nitrate requires direct charge transfer. Thus, the hydrogenation contribution may be important in expediting the reduction kinetics of formed nitrite, which may explain the lower nitrite accumulation observed for Cu/Co electrodes.

[0048] The possibility of NH_3 oxidation to produce NO_x gases was tested with a solution containing NH_4^+ with 30 mg-N L^{-1}. NH_4^+ oxidation was not sufficient to explain the increase of nitrogen gas species. No reoxidation to NO_3^- was observed during nitrite and ammonia experiments.

Assessing Ammonia Production and Electrode Stability

[0049] The performance of the electrocatalytic system to obtain NH_3 was evaluated in terms of kinetic constants and electrical figures of merit, such as Faradaic efficiency (FE) and electric energy per order (EE/O). As shown in FIG. **6***a*, the calculated pseudo-first order kinetic constant of Cu/Co of 6.0×10's^{-1} was 4.6 times higher than the observed for pristine Cu foam ($k_1=1.3\times10^{-4}$ s^{-1}). These results demonstrate the catalytic effect of Co sites that accelerate the nitrate abatement.

[0050] FIG. **4**A shows EE/O values of 10.2, 13.1, and 43.1 kWh m^{-3} $order^{-1}$ measured using Cu/Co, Cu—Pt and Cu foam materials, respectively. Under galvanostatic operation, the EE/O mainly depends on the observed cell potential and reduction kinetics. The observed cell potential is defined by the applied current density, but also by the ohmic resistance of the system and the electrode conductivity. Since tests are conducted under identical solution conditions (i.e., nitrate concentration, pH, and conductivity) the slight differences observed should be mostly related to material conductivity. Thus, cell potentials at 20 mA cm' were of the same order of magnitude with values of $E_{cell,\ Cu\ foam}=9.5$ V, $E_{cell,\ Cu/Pt}=8.8$ V and $E_{cell,\ Cu/Co}=9.8$ V. According to the EE/O definition by Eq. 3, the main EE/O driver would be the different kinetic rate. Cu/Co shows the highest competitiveness given the enhanced electrocatalytic performance on nitrate conversion kinetics.

[0051] Ammonia production is reported as ammonia yield (mmol NH_3 g_{cat}^{-1} h^{-1}) which is a quantitative parameter to evaluate and compare yield. As displayed in FIG. **4**B, Cu foam, Cu/Pt, and Cu/Co yielded an ammonia yield of 0.5 mmol NH_3 g_{cat}^{-1} h^{-1}, 0.6 NH_3 g_{cat}^{-1} h^{-1}, and 0.7 mmol NH_3 g_{cat}^{-1} h^{-1}, respectively. These results indicate that Cu/Co can be a more effective electrode for the production of ammonia than electrodes made using PGM-based materials. Ammonia yield may depend on the initial nitrate concentration. For example, the same electrode using different initial nitrate concentrations can obtain different ammonia yields since can affect the surface coverage ratio between adsorbed N-species and monoatomic hydrogen. A meaningful performance indicator is the percentage of ammonia production referred in terms of the maximum theoretical expected from the initial concentration of nitrate. Maximum ammonia production (100%) would be attained if all initial nitrogen concentration converts to ammonia. FIG. **4**B depicts increasing values of ammonia production percentage of 63, 75, and 87% for Cu foam, Cu/Pt, and Cu/Co, respectively. The same tendency is followed by the FE, where the highest efficiency of 20.7% is attained by the Co-nanocomposites, which is 2.0 times higher than the bare Cu foam.

[0052] These results indicate that Cu/Co is an alternative to electrocatalysts that rely on the use of PGMs. The Cu/Co nanocomposite can surpass the yield of Pt and Pt-nanoenabled electrodes (e.g., Cu/Pt). Eliminating the use of plati-

num group elements can minimize electrode capital expenditures while increasing the sustainability of the process.

[0053] Electrode activity and stability can serve as a basis to determine the feasibility of scaling-up of the electrocatalytic systems. Five sequential feed-batch trials were performed to evaluate the sustained performance of the electrode under continuous operation. Fresh synthetic solutions containing nitrate were consecutively treated during 120 minutes under the same operating conditions. The effectiveness of the Cu/Co electrode was evaluated in terms of nitrate conversion and metal leaching after the five reuses. FIG. **5**A shows the nitrate final conversion remained statistically unchanged (~98% removal) throughout the trials, demonstrating repeatability of the results over time with similar stable kinetics rate.

[0054] Metal leaching to aquatic environments poses a contamination risk and is preferably minimized when using multimetallic catalysts for water treatment. As reported by the National Primary Drinking Water Regulations (NPDWR), which is regulated by the United States Environmental Protection Agency (EPA), 1.3 mg L^{-1} is the maximum concentration level (MCL) for copper. Similar levels are set according to the Emission standard pollutants for cobalt with an MCL of 1.0 mg L^{-1} (Republic of China GB25467-2010). FIG. **5**B shows that the quantity of Cu (0.088-0.137 mg Cu L^{-1}) and Co (0.01-0.025 mg Co L^{-1}) leached after each use is significantly lower than the MCL by several orders of magnitude for both metals. The electrodeposition method disclosed herein provides a strong attachment between material interfaces that is superior to physical attachment obtained by common drop casting. The method can generate stable nanoenabled electrodes for sustained performance of nitrogen management electrified systems.

[0055] FIGS. **7**A-**7**D are scanning electron microscope (SEM) images of different bimetallic electrodes showing morphological characterization, of Cu/Co, Cu/Cu, Cu/Ni, and Cu/Sn, respectively.

[0056] FIGS. **8**A-**8**D show electrochemical reduction of nitrate with the evolution of nitrate, ammonia, and nitrogen gas.

[0057] FIG. **9** shows selectivity toward ammonia from the electrochemical reduction of nitrate at different current intensities.

[0058] Although this disclosure contains many specific embodiment details, these should not be construed as limitations on the scope of the subject matter or on the scope of what may be claimed, but rather as descriptions of features that may be specific to particular embodiments. Certain features that are described in this disclosure in the context of separate embodiments can also be implemented, in combination, in a single embodiment. Conversely, various features that are described in the context of a single embodiment can also be implemented in multiple embodiments, separately, or in any suitable sub-combination. Moreover, although previously described features may be described as acting in certain combinations and even initially claimed as such, one or more features from a claimed combination can, in some cases, be excised from the combination, and the claimed combination may be directed to a sub-combination or variation of a sub-combination.

[0059] Particular embodiments of the subject matter have been described. Other embodiments, alterations, and permutations of the described embodiments are within the scope of the following claims as will be apparent to those skilled in the art. While operations are depicted in the drawings or claims in a particular order, this should not be understood as requiring that such operations be performed in the particular order shown or in sequential order, or that all illustrated operations be performed (some operations may be considered optional), to achieve desirable results.

[0060] Accordingly, the previously described example embodiments do not define or constrain this disclosure. Other changes, substitutions, and alterations are also possible without departing from the spirit and scope of this disclosure.

What is claimed is:

1. A nanocomposite electrode comprising:

a porous copper substrate; and

Co_3O_4 and/or $Cu/Co(OH)_x$ nanoparticles electrolytically deposited on the porous copper substrate.

2. The electrode of claim **1**, wherein an average size of the Co_3O_4 and/or $Cu/Co(OH)_x$ nanoparticles is in a range of 50 nm to 500 nm.

3. The electrode of claim **1**, wherein the porous copper substrate is a copper foam.

4. The electrode of claim **3**, wherein a porosity of the copper foam is in a range of 5 to 200 pores per inch.

5. The electrode of claim **1**, wherein the Co_3O_4 and/or $Cu/Co(OH)_x$ nanoparticles extend from pore surfaces of the porous copper substrate.

6. The electrode of claim **1**, wherein the Co_3O_4 and/or $Cu/Co(OH)_x$ nanoparticles are bound to the porous copper substrate.

7. The electrode of claim **1**, wherein a volume of the nanocomposite electrode is at least 0.1 cm^3.

8. A method of making a nanocomposite electrode, the method comprising:

contacting a porous copper substrate with a solution comprising cobalt; and

electrodepositing the cobalt on the porous copper substrate to yield the nanocomposite electrode.

9. The method of claim **8**, wherein the porous copper substrate is a copper foam.

10. The method of claim **8**, wherein the solution comprises a cobalt salt in a range of 0.1 mol L^{-1} to 5 mol L^{-1}.

11. The method of claim **10**, wherein the solution comprises boric acid in a range of 0.1 mol L^{-1} to 5 mol L^{-1}.

12. The method of claim **11**, wherein the solution comprises sodium sulfate in a range of 0.01 mol L^{-1} to 1.0 mol L^{-1}.

13. The method of claim **8**, wherein electrodepositing the cobalt on the porous copper substrate comprises forming Co_3O_4 and/or $Cu/Co(OH)_x$ nanoparticles on surfaces of the porous copper substrate.

14. The method of claim **8**, wherein an average size of the Co_3O_4 and/or $Cu/Co(OH)_x$ nanoparticles is in a range of 50 nm to 500 nm.

15. A method of reducing nitrate to ammonia, the method comprising:

contacting the nanocomposite electrode of claim **1** with an aqueous solution comprising nitrate; and

electrocatalytically reducing the nitrate to yield ammonia.

16. The method of claim **15**, further comprising electrocatalytically reducing the nitrate to yield nitrite, and electrocatalytically reducing the nitrite to yield ammonia.

17. The method of claim **16**, wherein electrocatalytically reducing the nitrate to yield nitrite is facilitated by copper in the porous copper substrate.

18. The method of claim **17**, wherein electrocatalytically reducing the nitrite to yield ammonia is facilitated by cobalt in the cobalt nanoparticles.

* * * * *